Degradation of Polystyrene by Shear Stress in Isopropylphenyl Phosphate Solution*

MILOŠ NETOPILÍK and MIROSLAV KUBÍN, *Institute of Macromolecular Chemistry, Czechoslovak Academy of Sciences, 162 06 Prague 6, Czechoslovakia,* GÜNTHER SCHULTZ, *Zentralinstitut für Organische Chemie, Akademie der Wissenschaften der DDR, 1199 Berlin-Adlershof, German Democratic Republic,* JIŘÍ VOHLÍDAL, *Department of Physical Chemistry, Charles University, Albertov 2030, 128 40 Prague 2, Czechoslovakia,* IVO KÖSSLER and PAVEL KRATOCHVÍL, *Institute of Macromolecular Chemistry, Czechoslovak Academy of Sciences, 162 06 Prague 6, Czechoslovakia*

Synopsis

The molecular weight distribution functions of polystyrene degraded by shear stress in isopropylphenyl phosphate solution were compared with the calculated ones, obtained by assuming that up to a certain distance from each chain end the probability of bond scission is zero. Two phenomenological models were proposed for the probability of degradation in the central part of the chain. A comparison with experimental data suggests that the probability of degradation increases towards the center of the chain. Branched fractions formed by degradation in the presence of air were found to be present by the GPC method with on-line viscometric detection.

INTRODUCTION

Shear degradation by flow of polymers in solution continues to be intensively studied. The effect of the solvent has been investigated in considerable detail: Substantial degradation takes place particularly in thermodynamically poor solvents[1,2] apparently because intersegmental interaction is stronger here than in polymers dissolved in good solvents. Especially near the boundary of phase instability, the flow can induce phase separation,[3] leading to "dry friction" between individual segments of the polymer chain.[4] It is also known that under otherwise identical conditions the extent of degradation rapidly increases above a certain critical polymer concentration.[1,5]

Little is as yet known about the actual mechanism governing the process; it is apparently quite complex and involves probably the formation of intermolecular and intramolecular entanglements, obviously aided by strong intersegmental interactions.

The mechanism of degradation is closely associated with both the distribution of probability of bond scission along the chain and the breakage probability of macromolecules of different length in a polydisperse polymer. The time

*Dedicated to Professor O. Wichterle on the occasion of his 75th birthday.

Journal of Applied Polymer Science, Vol. 40, 1115–1130 (1990)
 CCC 0021-8995/90/07-81115-16$04.00

dependence of degradation has been shown[6,7] to obey the expression

$$\frac{dB_t}{dt} = k(B_\infty - B_t) \tag{1}$$

where k is a rate constant and B_t is the scission index defined as

$$B_t = M_{n0}/M_{nt} - 1 \tag{2}$$

M_{n0} is the original number-average molecular weight and M_{nt} refers to time t. For $M_{nt} = M_{n\infty}$ (where $M_{n\infty}$ is the number-average molecular weight after infinite time of degradation) we have $B_t = B_\infty$.

Equation (1) involves the implicit assumption that the final degradation product is a polymer with a certain limiting chain length[8] which indicates a similarity of degradation by flow and by ultrasound[9] and is equivalent to the assumption that the probability of rupture of a given bond remains zero up to a certain limiting distance ξ of the bond from the nearest chain end.

It is, however, apparent that the evaluation of experimental data on the basis of eq. (1) cannot provide detailed information on the mechanism of the process: All bonds in all chains of a polydisperse polymer must be taken into account at the given stage of degradation when the molecular weight distribution (MWD) of the degradation product is to be calculated exactly. The Simha equation,[10] which describes how the mole fraction $n(P, t)$ of polymer chains with degree of polymerization P varies with time t,

$$\frac{\partial n(P, t)}{\partial t} = -n(P, t)\int_0^P k(P, p)\,dp + 2\int_P^\infty k(Z, P)n(Z, t)\,dZ \tag{3}$$

can form the basis of such calculation. The rate constant $k(P, p)$ represents the probability that a chain of length P will rupture at a distance p from one chain end; eq. (3) involves the assumption that both directions along the chain are equivalent.

Several methods have been proposed for solving eq. (3); the most promising is that developed by Ballauf and Wolf[11] on the basis of a method developed by Basedow et al.,[12] who solve (3) as a set of discrete equations by matrix calculus.

The distribution of probability of chain scission along a polymer chain of a given length can in principle be determined by comparing the experimental MWD curves with functions calculated for different, judiciously selected breakage probabilities. Such attempts were indeed successful for polymers degraded by extensional flow. As shown by theoretical considerations concerning the conformation of polymers subject to elongational flow,[13] only midpoint scission of the longest chains occurs under these conditions, and maxima corresponding to halving of the highest fraction present in the sample were indeed observed on chromatograms of polymer degraded by elongational flow.[14,15] On the other hand, although some experiments with shear degradation of polymers by turbulent flow[5,6] indicated the prevalence of midpoint scission, other investigators[16] denied the existence of chain halving because they were unable to find the typical maxima on the chromatograms of

polymers degraded even if the starting polymer samples were of low polydispersity (M_w/M_n = 1.1–1.43). The rotational components of velocity in turbulent flow probably limit the elongation of polymer coils, so that the stress concentrates in the so-called grip points[4] in contrast to the situation prevailing in extensional flow, where mostly uncoiled, fully extended macromolecules undergo degradation.[14,15]

Hence, we must admit that the probability of scission in the central region of the macromolecule (at a distance larger than the limiting length ξ) is distributed in an unknown manner, and the same holds true about the probability that a chain of given length will rupture. Since the starting polymer is usually polydisperse, it is obvious that the calculation of MWD of the degraded sample requires the knowledge of a number of parameters (at least the minimum width of the breakage probability density along the chain and the probability that a polymer of a given length will break).

In this study we attempt to show to what extent it is possible to clarify the degradation mechanism by studying the effect of the assumed probability density of scission in the central part of the macromolecule on the molecular weight distribution of the degraded polymer, calculated by an approximate numerical method. The more advanced stages of the process, where degradation stops owing to the assumed existence of the limiting distance ξ, are discussed separately. The results of calculations are confronted with molecular weight distributions determined experimentally for polystyrene samples dissolved in isopropylphenyl phosphate, a system which finds practical application as a replacement for the noninflammable lubricants based on toxic chlorinated biphenyls.

THEORETICAL

Two model breakage probabilities were selected in order to throw light on the mechanism of degradation and to evaluate the effect of the distribution of scission probability along the macromolecule on the molecular weight distribution of the degraded polymer. Both models include the assumption that the breakage probability described by the rate constant $k(P, p)$ in eq. (3) is zero up to a certain distance ξ from the nearest chain end. In the first (rectangular) model it is assumed that the probability of rupture of a bond in the central region depends neither on its position in the chain nor on the chain length. Geometrically, this distribution represents a rectangle with base $P - 2\xi$ and height $k(P, p) = \text{const}$, and physically it corresponds to macromolecules which are cleaved mostly in the coiled conformation, where the difference between bonds situated near the chain end and the central bonds is small.

In the second (triangular) model, the probability that a given bond will break is taken to be proportional to its distance from the nearest chain end. Geometrically this distribution is a triangle with base P and height $k(P, p) \propto p$ but with two triangular parts of base length ξ near the lower edges removed. In the latter model, the macromolecules are assumed to rupture mostly in the extended conformation, where the force responsible for bond scission is a resultant of forces acting on individual chain segments. In both instances, the limiting length ξ is defined as that distance where the

resultant of forces exceeds the bond strength; naturally, both models simplify the actual situation to a considerable extent.

The molecular weight distributions of the starting polymers were modelled by the Schulz–Zimm functions[17] and the distribution of the degraded polymer was calculated numerically (at each of the 240 points defining the starting distribution) from the time variation $\partial n(P, t)/\partial t$ according to eq. (3). For distributions defined on a dense grid in M, used in this study, the above procedure proved to be simpler and more rapid than the exact method developed by Ballauf and Wolf.[11]

However, the employed procedure can lead to some errors in the final stages of degradation. In view of the fact that the molecular weight distribution of polymers degraded to such large extent is practically independent of the starting MWD, we shall first estimate the polydispersity of such degraded polymers independently.

Since we postulate that chains of length $P < \xi$ are not produced, their existence may be neglected and only chains with length between ξ and 2ξ may be considered. The sample which contains only chains of length ξ (with mole fraction n_ξ) along with chains of length 2ξ [with mole fraction $(1 - n_\xi)$] exhibits the highest polydispersity. According to the definition

$$P_m = \sum_i n_i P_i^m \Big/ \sum_i n_i P_i^{m-1} \tag{4}$$

(where for $m = 1$ and 2 we obtain expressions for P_n and P_w, respectively), for the sample under consideration we may write

$$P_n = (2 - n_\xi) \tag{5}$$

and

$$P_w = (4 - 3n_\xi)\xi/(2 - n_\xi) \tag{6}$$

For instance, for $n_\xi = 0.5$ we obtain from eq. (5) $(P_n)_{\text{deg}} = (3/2)\xi$, which formally agrees with the result obtained by Ovenall et al.[18] for a polymer degraded by ultrasound. By calculating P_w/P_n from the last equations and putting derivatives of this expression with respect to n_ξ equal to zero, we obtain for $n_\xi = 2/3$ the maximum value of P_w/P_n for this sample:

$$(P_w/P_n)_{\text{deg}} = (M_w/M_n)_{\text{deg}} = 9/8 = 1.125 \tag{7}$$

EXPERIMENTAL

Polystyrene samples were prepared by suspension radical polymerization at 73°C with potassium peroxodisulfate as the initiator. In the preparation of sample *g*, branching was achieved by adding 0.023% divinylbenzene (related to styrene). Both the starting samples and the degradation products were characterized at 25°C by light scattering in toluene solution in a Sofica apparatus ($\lambda = 546$ nm, $dn/dc = 0.111$ cm^3/g[19]) and viscometrically in butanone solution (constants of the Mark–Houwink equation $[\eta] = KM^a$ were[19] $K = 3.9 \times 10^{-2}$ cm^3/g, $a = 0.58$), in toluene (constants[20] $K = 1.16 \times 10^{-2}$ cm^3/g,

TABLE I
Molecular Weights of Polystyrene Samples

Sample	$M \times 10^{-5}$	Method,[a] solvent[b]	Sample	$M \times 10^{-5}$	Method,[a] solvent[b]
a	0.22	V, t	f	7.65	V, t
b	0.82	V, t		6.65	V, b
	0.79	V, b		8.78	LS, t
c	1.70	V, t	g[c]	11.6	V, t
	1.28	V, b		11.4	V, b
d	2.07	V, t	h	12.6	V, t
	1.90	V, b		11.8	V, b
	0.83	O, t	i	13.8	V, t
e	5.47	V, t		12.2	V, b
				13.5	LS, t

[a]Methods were light scattering (LS), viscometry (V), and osmometry at 25°C.
[b]Solvents were toluene (t) and butanone (b).
[c]Sample g was partly branched.

$a = 0.72$), and in tetrahydrofuran (constants[21] $K = 1.25 \times 10^{-2}$ cm^3/g, $a = 0.713$) (Table I).

In gel permeation chromatography (GPC), the polymer concentration in the eluate was measured (by a Waters differential refractometer) along with the viscosity of the eluent. Four columns with a diameter 8 mm and length 1.2 m were used. To characterize the initial samples and samples degraded in the presence of air, the columns were packed with Merckogel Si gels (Merck), porosity 500, 100, 50, and 20 nm, particle size 40–63 μm. Butanone was the mobile phase at a flow rate of 0.15 mL/min. To characterize samples degraded in the absence of oxygen, the columns were packed with a copolymer of styrene and divinylbenzene; the molecular weight exclusion limits were 1.7×10^6, 5×10^5, 10^4, and 10^3. In this case tetrahydrofuran was the mobile phase (flow rate = 0.5 mL/min). The viscometric detector was a capillary viscometer (capillary diameter 0.35 mm) provided with a siphon (1.71 mL) with photoelectric detection and recording of flow times. The flow time of pure solvent (butanone) at 25°C was $t_0 = 62$ s. From the recorded flow times t and the flow time of pure solvent t_0, the quantity[22]

$$(c[\eta])_V = \sqrt{2}\sqrt{t/t_0 - 1 - \ln(t/t_0)} \tag{8}$$

was calculated as a function of elution volume. The concentration was calculated from the chromatogram W_V at a given elution volume V using the formula

$$c_V = W_V \frac{\int (c[\eta])_V \, dV}{[\eta] \int W_V \, dV} \tag{9}$$

where $[\eta]$ is the intrinsic viscosity of the unfractionated sample. The integration (Simpson's rule) was performed over the whole chromatogram. Both

quantities c_V and $(c[\eta])_V$ were simultaneously corrected for axial dispersion by a procedure[23] based on the numerical method of Pierce and Armonas.[24] The spreading factors for the two separation systems ($h = 0.47$ for Merckogel Si and $h = 0.35$ for the styrene–divinylbenzene packing) were determined from the requirement that the slope of the dependence of $\log M$ on elution volume, calculated from the spreading-corrected data at the chromatogram peak, must coincide with the slope of the calibration curve. The intrinsic viscosity of the polymer was determined as a function of elution volume V by forming the ratio of both corrected functions, $(c[\eta])_V$ and c_V.

If branching was detected in the degraded samples (this happened also in those cases where the starting polymer was linear), the molecular weight was calculated from the formula

$$M = M_c[\eta]_{l,V}/[\eta]_{b,V} \tag{10}$$

where M_c is the molecular weight determined from the calibration dependence and the subscripts l, V and b, V refer to a linear and branched polymer, respectively, which leave the column at the same elution volume V; the quantity $[\eta]_{l,V}$ may be calculated from the molecular weight given by calibration. The validity of eq. (10) is based on the assumption of the so-called universal calibration.[25] The extent of branching was estimated from the factor

$$g = [\eta]_{l,M}/[\eta]_{b,M} \tag{11}$$

(where the intrinsic viscosity values of the branched and linear polymer refer to the same molecular weight) calculated from the relation[21]

$$g = \left([\eta]_{l,V}/[\eta]_{b,V}\right)^{1+a} \tag{12}$$

where a is the exponent of the Mark–Houwink equation for the linear polymer and the intrinsic viscosities refer to the same elution volume V.

Degradation of the polymer was carried out in an apparatus built according to the standard DIN 51 382, in which degradation is achieved by periodically passing the polymer solution through a nozzle (Fig. 1). The force of the nozzle spring was adjusted so as to make it open at 17.5 MPa. In order to determine the circulation number C (defined as the number of passages of the total volume—200 mL of solution—through the nozzle), the apparatus was provided with a counter of pump motor revolutions. The polymer concentration was always $c = 1.18 \times 10^{-2}$ g/cm^3. Technical grade isopropylphenyl phosphate was the solvent.

RESULTS AND DISCUSSION

Numerical Calculations

To determine the properties of both models described in the theoretical part, we chose $P_w = 35.3$ and $P_w/P_n = 1.2$, 2, and 2.5 for the starting distribution functions. The chosen limiting length was $\xi = 11$ and, for the sake of comparison, also $\xi = 0$. Both the triangular and rectangular model yield very

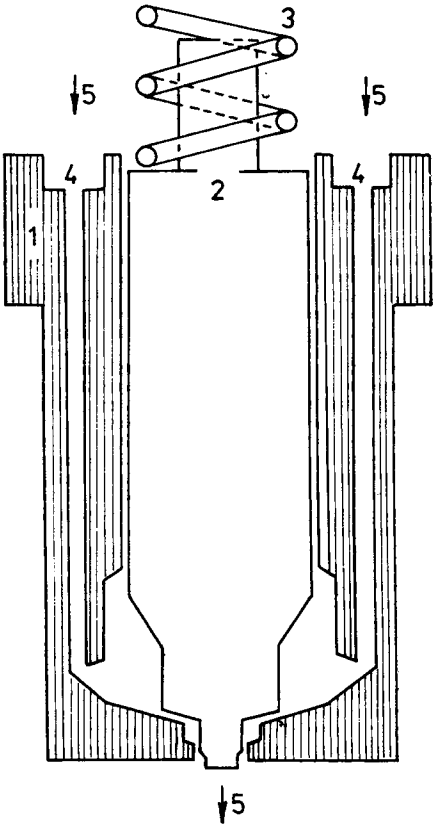

Fig. 1. Schematic cross section through the injection nozzle: (1) body of the nozzle; (2) piston; (3) spring; (4) supply of liquid; (5) direction of flow.

similar results for the average degrees of polymerization and polydispersity (Fig. 2); the variable $\log(t' + 1)$ was introduced in order to accentuate the shape of the curves, and also to make the axis of the independent variable start from zero. The limiting length ξ is obviously decisive for the shape of the time dependence. If $\xi = 0$ [Fig. 2(a), broken curves], in the advanced stages of calculation the calculated time dependences of P_w/P_n approach each other closely. This case corresponds to random degradation. When a chain may be degraded to arbitrarily small parts, polydispersity of the product approaches[26] $P_w/P_n = 2$. This also approximately holds in the reported case at the beginning of degradation, as long as the length of the segment not undergoing degradation is small in comparison with the mean chain length. Accordingly, the width of the calculated distribution increases in those cases where the starting value of P_w/P_n is smaller than 2, while in the opposite case it decreases from the very beginning. In advanced stages of the process the length of the limiting segment can be no longer neglected and the calculated polydispersity therefore begins to approach $P_w/P_n = 1$, a theoretical value corresponding to a polymer degraded to individual segments.

At $\xi = 11$ both the shape of the time dependence and the final values of P_w/P_n are seen to depend strongly on the width of the initial distribution. In

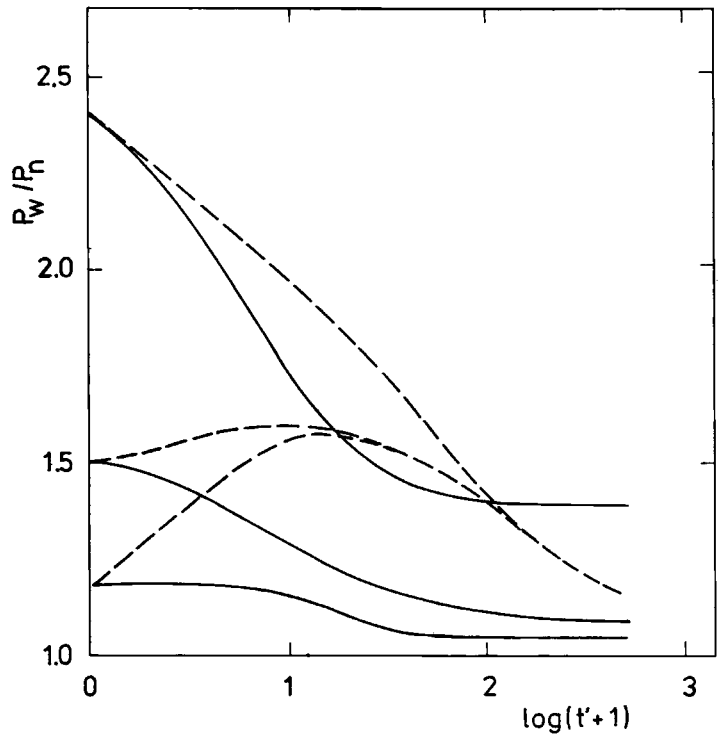

(a)

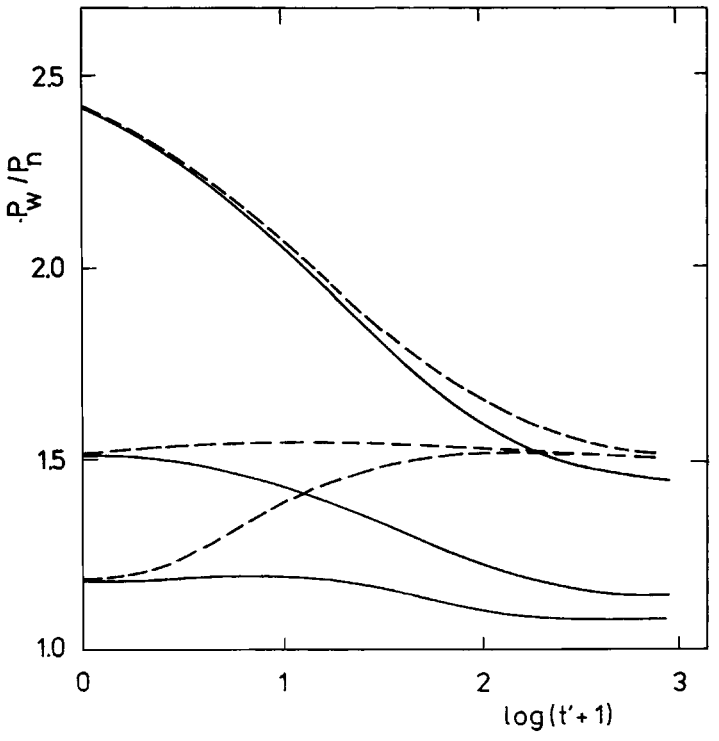

(b)

Fig. 2. The ratio P_w/P_n for three model polymers with the starting value $P_w = 35.3$, calculated for the rectangular (a) and triangular (b) model as a function of $\log(t' + 1)$ (where t' is the relative time). The limiting length $\xi = 11$ (solid curves) and $\xi = 0$ (broken curves).

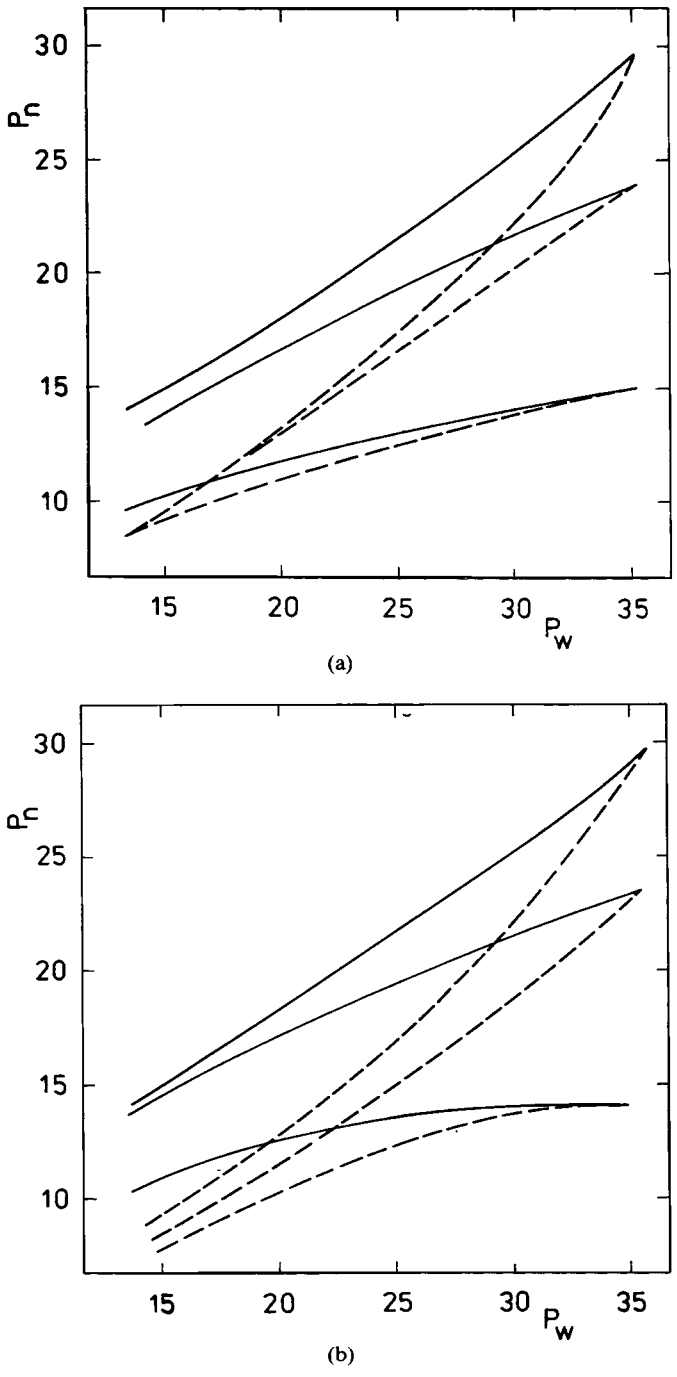

Fig. 3. Typical P_n vs. P_w dependences calculated for starting polymers with $P_w = 35$; limiting length $\xi = 11$ (solid curves) and $\xi = 0$ (broken curves) for the triangular (a) and rectangular (b) model.

the case of relatively narrow distributions (P_w/P_n = 1.2 and 2) the resulting polydispersity is low, in agreement with the maximum possible value of P_w/P_n = 1.125 given by eq. (7). When the polydispersity of the starting polymer is large, the presence of chains shorter than ξ leads to a final product with polydispersity much higher than the theoretical limiting value. No fundamental difference can be found between curves calculated using the triangular and the rectangular model. Since in this case the average chain length of the degradation product greatly exceeds the segment length, this conclusion holds also for a high-molecular-weight polymer.

A comparison between the calculated dependences and the experiment is complicated by the fact that the phenomenological models describe the degradation in terms of a time parameter which is not equal but merely proportional to real time. On the other hand, the dependence (Fig. 3) between P_n and P_w during the degradation process (where the time parameter has been eliminated) allows a direct comparison with the experiment: the dependences for both models are similar; with $\xi = 11$, the P_n values are higher than at $\xi = 0$, in agreement with the expected narrowing of the distribution.

Degradation Experiments

With proceeding degradation, the molecular weight of the degraded polymers approached the values $(M_n)_\infty = 4.7 \times 10^4$ and $(M_\eta)_\infty = 8.5 \times 10^4$; these values, corresponding to infinite time of degradation, were estimated by extrapolating linearly M_n and M_η to $\log(C^{-1} + 1) \to 0$ (i.e., for the circulation number C approaching infinity). Let us now use the resulting value of $(M_n)_\infty$ for checking the validity of eq. (1). Integrating (1) with an integration constant equal to $\ln(B_0 - B_\infty)$, we arrive at the formula

$$\ln \frac{B_t - B_\infty}{B_0 - B_\infty} = -kt \tag{13}$$

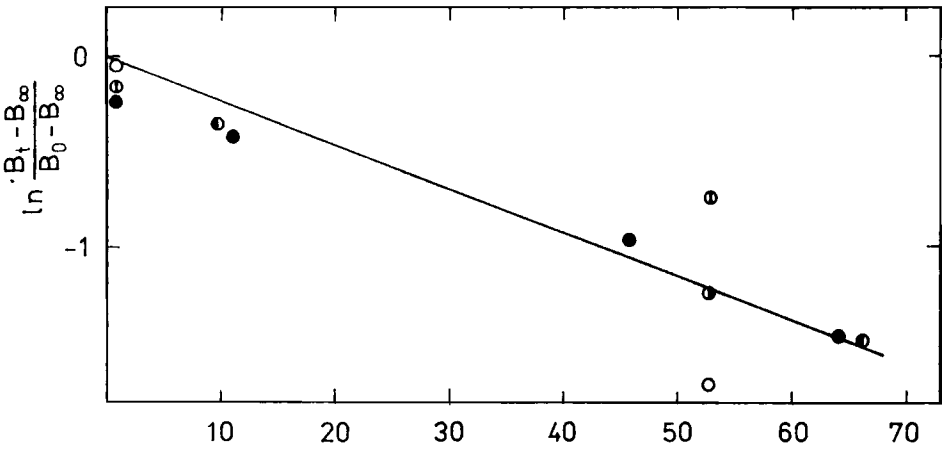

Fig. 4. Time dependence of the extent of polystyrene degradation, plotted accordingly to eq. (13). The circulation number C is used as the independent variable instead of time; samples a (○), b (⦶), c (◑), d (◐), and e (●).

TABLE II
Results of GPC Analysis of Polystyrene Samples Degraded in the Nozzle

C[a]	$M_n \times 10^3$	$M_w \times 10^3$	M_w/M_n	$[\eta]_{GPC}$[d] (cm^3/g)	$[\eta]$[e] (cm^3/g)	g[f]
			Sample d			
0[b]	70	218	3.11			
1[c]	73	185	2.54	70	43	0.43
52.5[c]	54	107	1.99	48	43	0.83
			Sample f			
0[b]	150	600	4.00			
1[c]	124	304	2.45	102	88	0.78
52.5[c]	75	127	1.69	55	44	0.60
			Sample g			
0[b]	151	1530	10.13			
1[c]	121	340	2.81	108	81	0.61
52.5[c]	63	115	1.83	51	44	0.78
			Sample h			
0[b]	215	1190	5.53			
1[c]	150	377	2.51	117	74	0.46
9.4[c]	111	191	1.72	74	62	0.74
66.2[c]	61	105	1.72	50	55	—
			Sample i			
0[b]	271	1390	5.13			
1[c]	141	360	2.55	114	97	0.70
11.7[c]	110	206	1.87	77	62	0.89
45.7[c]	74	141	1.91	60	56	0.89
63.9[c]	62	107	1.73	48	40	0.73

[a] C = circulation number in the nozzle.
[b] Butanone was used for the analyses of the starting samples (C = 0).
[c] Tetrahydrofurane was used for the analyses of degraded samples.
[d] Intrinsic viscosity values $[\eta]_{GPC}$ were calculated from chromatogram and calibration dependence of the column.
[e] Intrinsic viscosity values $[\eta]$ were measured independently in an Ubbelohde viscometer.
[f] Factor g defined by eq. (11) was calculated using eq. (12).

which describes the extent of degradation of a given polymer as a function of time, regardless of the shape of the starting MWD (see Fig. 4, where the circulation number C is used instead of t as the independent variable).

In accord with Ref. 16, the registered chromatograms of degraded polymers did not exhibit distinct peaks at some lower values of M (in contrast to the case of degradation by extensional flow, where the stress leads essentially to midpoint scission). The nonuniformity continued to decrease during the degradation (Table II). The lowering of nonuniformity agrees with the theory but the predicted limiting value $(M_w/M_n)_{deg} = 1.125$ was never attained in our experiments.

The limiting molecular weight $M_\xi = 31.3 \times 10^4$ (corresponding to the limiting distance ξ) was estimated as $M_\xi = (2/3)(M_n)_\infty$, where the factor (2/3) follows from eq. (5) for the mean value $n_\xi = 0.5$. (We assume that molecules of length between ξ and 2ξ are distributed uniformly in the degradation product.)

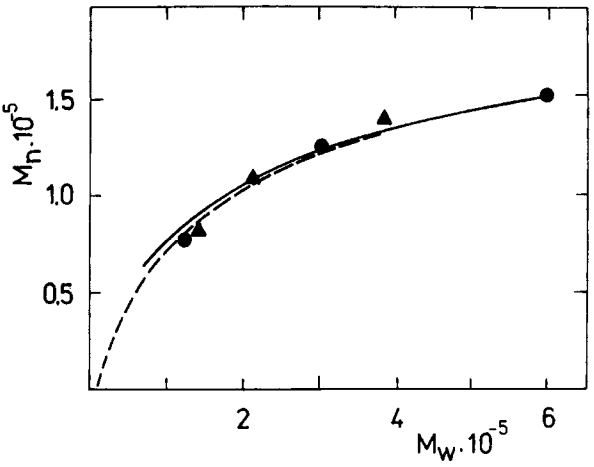

Fig. 5. Comparison of the M_n vs. M_w dependence during degradation of samples f (●) and i (▲) with results of the model calculation; triangular (solid curve) and rectangular (broken curve) model.

For a comparison of the model calculations with experiment, one cannot describe the molecular weight distribution of the sample with a precision corresponding to a single chain segment: A larger step in M is necessary, owing to machine time and memory limitations. Nevertheless, the dependence of M_n on M_w during degradation is described adequately (Fig. 5), in particular by the triangular model. Since the results for the rectangular model are only slightly different, we do not dare to decide definitely which of the two models fits the experimental data better.

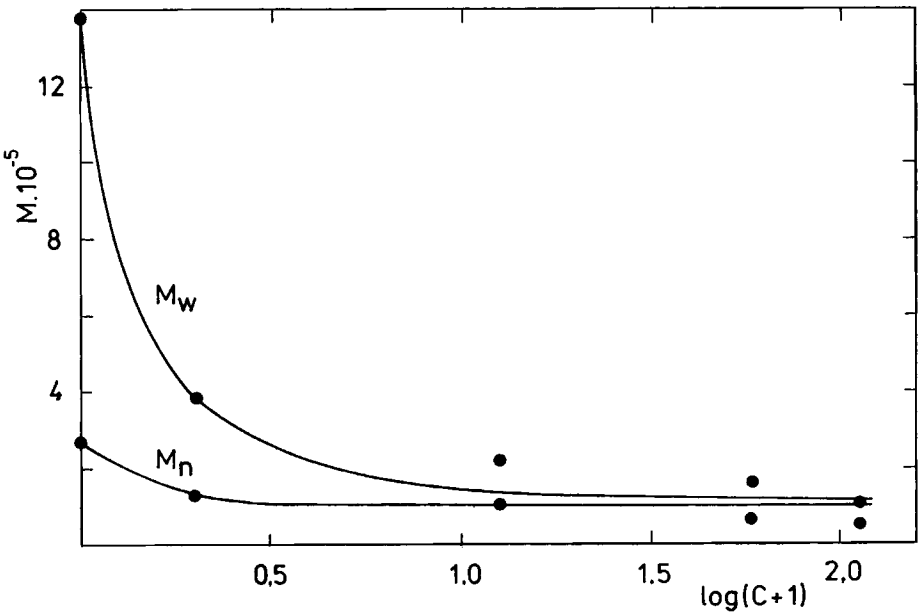

Fig. 6. Comparison of the time dependences of M_w and M_n during the simulated degradation (triangular model) with experimentally determined distribution functions for sample i.

With a suitably chosen time unit in model calculations, it is also possible to describe adequately the time dependences of M_w and M_n during degradation. Let us take the triangular model as an example (Fig. 6). The starting points are defined—they correspond to the initial distribution. The scales were adjusted by identifying the circulation number C of the most degraded polymer with a value of t' such that P_w and P_n were situated at roughly the same distance from the calculated curves.

Effect of Oxygen on Degradation

All intrinsic viscosity values of degraded polystyrene samples are lower than those calculated from chromatograms using the Mark–Houwink constants for linear polystyrene (Table II). This indicates that branching takes place during the degradation (probably due to air oxygen). With the adopted evaluation procedures the average intrinsic viscosity calculated from the combined detector records is identical with the viscosity of the unfractionated sample [cf. eq. (9)]. Since in this case the data of the viscometer do not provide additional information, we give only values of the g factor calculated using eq. (12) from

TABLE III
Results of GPC Analyses (Butanone as Eluent) of Samples Degraded in the Mixer

%	$M \times 10^{-3}$ M_n	M_w	M_w/M_n	%	$M \times 10^{-3}$ M_n	M_w	M_w/M_n
	Sample a				Sample f		
	68	147	2.16	14.4[a]	1880	2390	1.27
				14.4[a]	6533[d]	9480[d]	1.45[d]
	Sample b						
1.2[a]	2950	3490	1.18	85.6[b]	108	180	1.67
98.8[b]	21	91	4.33	100[c]	126	501	3.98
100[c]	21	130	6.19				
					Sample g		
				13.7[a]	5750	6634	1.15
	Sample c						
5.4[a]	2586	3150	1.22	86.3[b]	165	304	1.84
94.6[b]	44	177	4.06	100[c]	190	1171	6.16
100[c]	46	338	7.35				
					Sample h		
				2.6[a]	4640	4950	1.07
	Sample d						
	71	175	2.46	97.4[b]	159	251	1.58
				100[c]	163	373	2.89
	Sample e				Sample i		
15.5[a]	2562	3052	1.19				
15.5[a]	9578[d]	12421[d]	1.30[d]		120	213	1.77
84.5[b]	131	253	1.93				
100[c]	153	687	4.49				

[a] The percentage of high-molecular weight peak.
[b] The percentage of low-molecular weight peak.
[c] The whole chromatogram.
[d] Values calculated for the high-molecular weight peak from the on-line viscometer data using eq. (10).

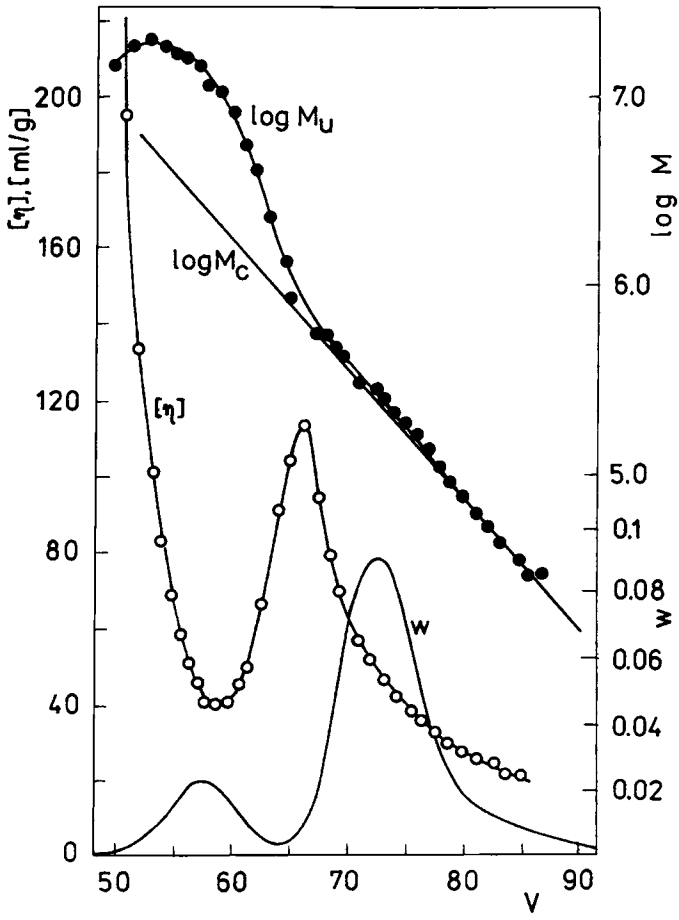

Fig. 7. Analysis of sample f degraded in the presence of air oxygen by GPC with on-line viscometric detection. The chromatogram height W, the intrinsic viscosity $[\eta]$ at 25°C, the calibration dependence for linear polystyrene log M_c, and the molecular weight log M_u calculated using eq. (10) are plotted against the elution volumes V; all functions corrected for axial dispersion.

the integral $[\eta]$ and M_η values (Table II) where M_η was calculated using the Mark–Houwink exponent for linear polystyrene.

To characterize the effect of oxygen, shear degradation was carried out with the polymer solution situated in a normal mixer (where a considerable amount of foam was formed). The time dependences of parameters characterizing the extent of degradation resembled those obtained in degradation experiments in the nozzle. Chromatograms of samples degraded to the final stage, where their molecular weight remained virtually constant, in most instances contained a high-molecular weight peak (Table III). If the peak was sufficiently high, it could be analyzed by GPC with the twin detection concentration–viscosity. In the region of the high-molecular weight peak the intrinsic viscosity dropped markedly (Fig. 7), probably due to strong branching. The molecular weight according to eq. (10) was higher than that determined from the calibration curve. The molecular weight averages calculated from GPC also considerably

TABLE IV
Intrinsic Viscosity Values $[\eta]$ at 25°C of the Samples Degraded in the Mixer

Sample	Butanone			Toluene	
	$[\eta]$ (cm^3/g)	$M_\eta \times 10^{-5}$[a]	g[b]	$[\eta]$ (cm^3/g)	$M_\eta \times 10^{-5}$[a]
a	—	—	—	15	0.22
b	—	—	—	38	0.76
c	35	1.24	0.64	60	1.44
d	44	1.83	—	73	1.89
e	49	2.20	0.51	80	2.15
f	49	2.20	0.68	83	2.26
g	51	2.37	0.39	91	2.57
h	52	2.44	0.87	88	2.45
i	51	2.36	—	84	2.29

[a] Viscosity average molecular weight corresponds to the linear polymer.
[b] Factor g defined by eq. (11) was calculated by using eq. (12).

exceeded those determined from intrinsic viscosities (Table IV). The factor g calculated using eq. (12) from the intrinsic viscosity of the sample (an average over the whole sample) varied from 0.6 to 0.8. Using the data of the on-line viscometer, we obtained for the high-molecular weight peak $g = 0.10$ for sample e and $g = 0.17$ for sample f. Such low values of g suggest considerable branching. One may assume that radicals R$^\cdot$ which arise by scission of the polymer may react with oxygen from air via the so-called peroxidation mechanism, observed, for example, with radicals produced during thermal degradation.[27] The reaction between the radical R$^\cdot$ and oxygen gives rise to the radical ROO$^\cdot$ which in turn produces a new radical by abstracting hydrogen from the polymer. This cyclic process, along with radical termination, may yield highly branched or even crosslinked structures.

CONCLUSIONS

Results of the theoretical analysis and of an experimental investigation of polystyrene degradation by shear stress in isopropylphenyl phosphate can be summarized as follows:

(i) Mechanical shear degradation by turbulent flow cleaves macromolecules mostly in the central region, at a distance from each chain end larger than a certain limiting length ξ. The molecular weight distribution of the degraded polymer is not very sensitive to the shape of the function selected to describe the probability of scission in the central region of the chain; accordingly, for a polydisperse starting polymer one cannot discriminate between the two models on the basis of molecular weight distribution measured for degraded polymers.

(ii) The kinetics of degradation induced by turbulent flow can be described over long time periods by a single master curve based on eq. (1).

(iii) Repeated scission of the dissolved polymer by shear stress causes narrowing of the distribution function. The theoretical limiting polydispersity value M_w/M_n was not attained in the experiments, however.

(iv) Degradation of polystyrene in the presence of air leads to the formation of branched products. Their presence was proved by the GPC method with on-line viscometric detection.

References

1. H. G. Müller and J. Klein, *Makromol. Chem.*, **182**, 3545 (1981).
2. A. F. Horn and E. W. Merrill, *Polym. Commun.*, **28**, 172 (1987).
3. H. Krämer and B. A. Wolf, *Makromol. Chem. Rapid. Commun.*, **6**, 21 (1985).
4. B. A. Wolf, *Makromol. Chem. Rapid Commun.*, **8**, 461 (1987).
5. E. W. Merrill and A. F. Horn, *Polym. Commun.*, **25**, 144 (1984).
6. M. Ballauf and B. A. Wolf, *Macromolecules*, **17**, 209 (1984).
7. F. K. Herold, G. V. Schulz, and B. A. Wolf, *Polym. Commun.*, **29**, 59 (1986).
8. A. Ram and A. Kadim, *J. Appl. Polym. Sci.*, **14**, 2145 (1970).
9. B. J. Coyne and H. H. G. Jellinek, *J. Polym. Sci.*, **A-2**, 633 (1967).
10. R. Simha, *J. Appl. Phys.*, **12**, 569 (1941).
11. M. Ballauf and B. A. Wolf, *Macromolecules*, **14**, 654 (1981).
12. A. M. Basedow, K. H. Ebert, and H. E. Ederer, *Macromolecules*, **11**, 774 (1978).
13. Y. Rabin, *J. Chem. Phys.*, **88**, 4014 (1988).
14. J. A. Odell, A. Keller, and M. J. Miles, *Polym. Commun.*, **24**, 7 (1983).
15. J. A. Odell and A. Keller, *J. Polym. Sci.*, **24**, 1889 (1986).
16. E. W. Merrill and P. Leopairat, *Polym. Eng. Sci.*, **20**, 1889 (1980).
17. B. H. Zimm, *J. Chem. Phys.*, **16**, 1093 (1948).
18. D. V. Ovenall, G. W. Hastings, and P. E. M. Allen, *J. Polym. Sci.*, **33**, 207 (1958).
19. J. Brandrup and E. H. Immergut, Eds., *Polymer Handbook*, 2nd ed., Wiley-Interscience, New York, London, Sydney, 1975.
20. V. Petrus, B. Porsch, B. Nyström, and L.-O. Sundelöf, *Makromol Chem.*, **183**, 1279 (1979).
21. W. S. Park and W. W. Graesley, *J. Polym. Sci. Polym. Phys. Ed.*, **15**, 71 (1978).
22. O. F. Solomon and I. Z. Ciuta, *J. Appl. Polym. Sci.*, **6**, 683 (1962).
23. M. Netopilík and G. Schulz, *Acta Polym.*, **35**, 140 (1984).
24. P. E. Pierce and J. E. Armonas, *J. Polym. Sci.*, **C1**, 23 (1968).
25. Z. Grubisic, P. Rempp, and H. Benoit, *J. Polym. Sci.*, **B5**, 753 (1967).
26. O. Saito, *J. Phys. Soc. Jpn.*, **13**, 198 (1958).
27. N. Grassie, *Chemistry of High Polymer Degradation Processes*, Butterworth, London, 1956.

Received December 28, 1988
Accepted April 13, 1989